Electronic phase separation in the rare-earth manganates $(La_{1-x}Ln_x)_{0.7}Ca_{0.3}MnO_3$ (Ln = Nd, Gd and Y)

2003 J. Phys.: Condens. Matter 15 3029

(http://iopscience.iop.org/0953-8984/15/19/306)

INSTITUTE OF PHYSICS PUBLISHING JOURNAL OF PHYSICS: CONDENSED MATTER

J. Phys.: Condens. Matter **15** (2003) 3029–3040 PII: S0953-8984(03)59392-4

Electronic phase separation in the rare-earth manganates $(La_{1-x}Ln_x)_{0.7}Ca_{0.3}MnO_3$ (Ln = Nd, Gd and Y)

L Sudheendra and C N R Rao

Chemistry and Physics of Materials Unit, Jawaharlal Nehru Centre for Advanced Scientific Research, Jakkur PO, Bangalore-560064, India

E-mail: cnrrao@jncasr.ac.in

Received 10 February 2003
Published 6 May 2003
Online at stacks.iop.org/JPhysCM/15/3029

Abstract

Electron transport and magnetic properties of three series of manganates of the formula $(La_{1-x}Ln_x)_{0.7}Ca_{0.3}MnO_3$ with Ln = Nd, Gd and Y, wherein only the average A-site cation radius $\langle r_A \rangle$ and associated disorder vary, without affecting the Mn^{4+}/Mn^{3+} ratio, have been investigated in an effort to understand the nature of phase separation. All three series of manganates show saturation magnetization characteristic of ferromagnetism, with the ferromagnetic T_c decreasing with increasing x up to a critical value of x, x_c ($x_c = 0.6$, 0.3, 0.2 respectively for Nd, Gd, Y). For $x > x_c$, the magnetic moments are considerably smaller, showing a small increase around T_M, the value of T_M decreasing slightly with increase in x or decrease in $\langle r_A \rangle$. The ferromagnetic compositions ($x \leqslant x_c$) show insulator–metal transitions, while the compositions with $x > x_c$ are insulating. The magnetic and electrical resistivity behaviour of these manganates is consistent with the occurrence of phase separation in the compositions around x_c, corresponding to a critical average radius of the A-site cation, $\langle r_A^c \rangle$, of 1.18 Å. Both T_c and T_{IM} increase linearly when $\langle r_A \rangle > \langle r_A^c \rangle$ or $x \leqslant x_c$, as expected of a homogeneous ferromagnetic phase. Both T_c and T_M decrease linearly with the A-site cation size disorder as measured by the variance σ^2. Thus, an increase in σ^2 favours the insulating AFM state. Percolative conduction is observed in the compositions with $\langle r_A \rangle > \langle r_A^c \rangle$. Electron transport properties in the insulating regime for $x > x_c$ conform to the variable-range hopping mechanism. More interestingly, when $x > x_c$, the real part of dielectric constant (ε') reaches a high value (10^4–10^6) at ordinary temperatures dropping to a very small (∼500) value below a certain temperature, the value of which decreases with decreasing frequency.

1. Introduction

Rare-earth manganates of the general formula $Ln_{1-x}A_xMnO_3$ (where Ln = rare earth, A = alkaline earth) exhibit many interesting properties such as colossal magnetoresistance, charge ordering and electronic phase separation [1–3]. Phase separation in these materials has attracted much interest in the last few years because of the fascinating features associated with the phenomenon [3]. Of the various manganite compositions, the $(La_{1-x}Pr_x)_{0.7}Ca_{0.3}MnO_3$ system has provided particularly valuable information on the electronic phase separation [4–6]. This is a convenient system for study of phase separation, since the Pr-rich compositions are antiferromagnetic (AFM) and charge ordered (CO), whereas the La-rich compositions are ferromagnetic metals (FMM). At a fixed Ca mole fraction of 0.3, a change in x leads to a transition from FMM behaviour to a charge-ordered insulator (COI) behaviour around an x-value of 0.7. That phase separation in $(La_{1-x}Pr_x)_{0.7}Ca_{0.3}MnO_3$ involves the FMM and COI domains has been demonstrated by various types of measurement. This system exhibits several unusual features. Thus, in spite of the drop in resistivity at the insulator–metal (IM) transition, the charge-ordered peaks in the x-ray diffraction pattern continue to grow at low temperatures [7]. Besides the COI phase, another phase is suggested to be present below the charge-ordering temperature [7]. On the basis of a neutron diffraction study, a phase diagram has been provided for this system wherein the $0.6 \leqslant x \leqslant 0.8$ region separates the homogeneous FMM and AFM phases [8].

Noting that the phase separation in $(La_{1-x}Pr_x)_{0.7}Ca_{0.3}MnO_3$ is triggered by A-site cation disorder, we considered it important to investigate a series of compounds of the type $(La_{1-x}Ln_x)_{0.7}Ca_{0.3}MnO_3$ over a range of compositions $0 \leqslant x < 1$ where the variation in Ln brings about a marked change in the average A-site cation radius, $\langle r_A \rangle$, as well as the size disorder. In this paper, we report the results of a systematic study of the electronic, magnetic and dielectric properties of three series of $(La_{1-x}Ln_x)_{0.7}Ca_{0.3}MnO_3$ with Ln = Nd, Gd and Y. It is to be noted that in all the compositions of the three series of manganates, the Mn^{4+}/Mn^{3+} ratio remains constant, the only variable being the average A-site cation radius and the associated disorder.

2. Experimental details

Compositions of the formula $(La_{1-x}Ln_x)_{0.7}Ca_{0.3}MnO_3$ (Ln = Nd, Gd or Y) were prepared by standard solid-state synthesis. A stoichiometric mixture of the rare-earth acetate, $CaCO_3$ and MnO_2 was mixed thoroughly in an agate mortar with the help of iso-propyl alcohol, and the mixture was first fired to 1273 K for 48 h with two intermediate grindings. This preheated sample was then further heated at 1473 K for 24 h, pressed into pellets and fired to 1648 K for 12 h to obtain the single-phase compounds. The samples were tested for phase purity by means of x-ray analysis using a Seifert 3000 diffractometer and the composition was checked by EDAX measurements. All the compositions were fitted to an orthorhombic unit-cell with the *Pnma* space group. The unit-cell dimensions of $(La_{1-x}Ln_x)_{0.7}Ca_{0.3}MnO_3$ decreased with increase in x in all the three series of compounds (figure 1), with a corresponding decrease in the unit-cell volume as expected when a large cation is replaced by a smaller cation. The dependence of the unit-cell dimensions and volume for three different compositions parallels the dependence of the average radius of the A-site cations, $\langle r_A \rangle$, on x. Thus a plot of the unit-cell volume for all the series against $\langle r_A \rangle$ is linear, as shown in the inset of figure 1.

Magnetization measurements were carried out in a Lakeshore vibrating sample magnetometer in the 300–50 K temperature range at an applied field of 4000 G. Electrical transport properties were measured by the standard four-probe method with silver epoxy as

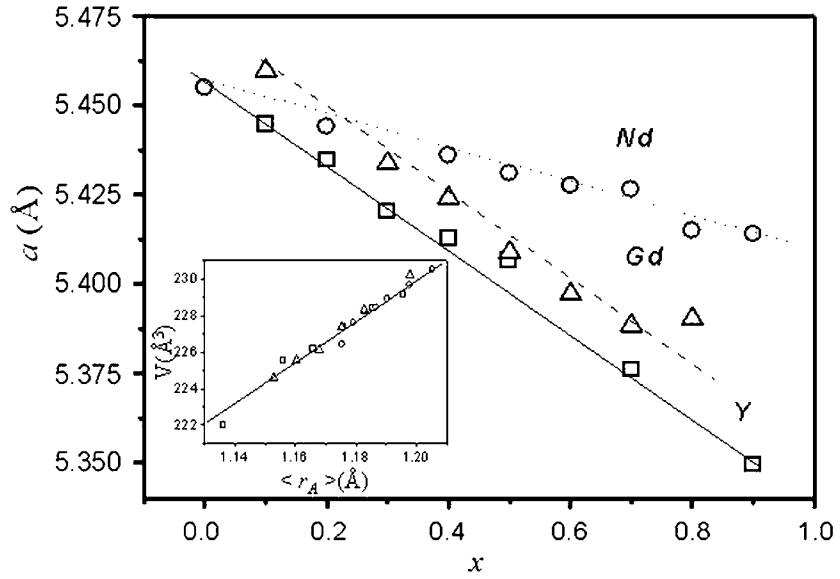

Figure 1. The variation of the unit-cell dimension a (Å) with x in $(La_{1-x}Ln_x)_{0.7}Ca_{0.3}MnO_3$. The inset shows the variation of the unit-cell volume with $\langle r_A \rangle$ (Å) in $(La_{1-x}Ln_x)_{0.7}Ca_{0.3}MnO_3$.

the electrodes in the 300–20 K temperature range. Dielectric measurements were carried out with the help of Agilent 4294A impedance analyser with gold coating on either side of the disc-shaped samples acting as electrodes. The data were collected from 85–300 K.

3. Results and discussion

In figure 2(a), we show the results of magnetic measurements on the $(La_{1-x}Nd_x)_{0.7}Ca_{0.3}MnO_3$ series, to show how the magnetic moment (μ_β) is sensitive to the substitution of the smaller Nd^{3+} cation in place of La^{3+}. We see a clear FM transition down to $x = 0.5$ with a saturation magnetic moment close to 3 μ_β. The ferromagnetic Curie temperature, T_c, shifts to lower temperatures with increase in x. We fail to see magnetic saturation in compositions with $x \geqslant 0.6$ and, instead, the maximum value of μ_β is far less than three at low temperatures. We designate the composition up to which ferromagnetism occurs as the critical composition x_c. The compositions with $x > x_c$ show a gradual, definitive increase in the magnetization or μ_β at a temperature T_M, the T_M-value decreasing with increasing x. It is possible that T_M represents the onset of canted antiferromagnetism (CAF). In $(La_{1-x}Gd_x)_{0.7}Ca_{0.3}MnO_3$, ferromagnetism is observed up to $x = 0.3$. T_c decreases with increase in x in the composition range $0.0 \leqslant x \leqslant 0.3$. For $x > 0.3$, we observe a gradual increase in the μ_β-value at low temperature around T_M, with the value of T_M decreasing with increase in x. Note that the value of x_c (∼0.3) in the Gd series is considerably lower than that in the Nd series where it was 0.6, showing that x_c decreases with the decrease in the average radius of the A-site cation, $\langle r_A \rangle$. The results for the $(La_{1-x}Gd_x)_{0.7}Ca_{0.3}MnO_3$ series of manganates (figure 2(b)) obtained by us agree with those reported for the $x = 0.0$–0.25 compositions by Terashita and Neumeier [9]. In $(La_{1-x}Y_x)_{0.7}Ca_{0.3}MnO_3$, ferromagnetism is seen only for compositions with $x \leqslant 0.2$, T_c decreasing with increase in x. Compositions with $x > 0.2$ show a gradual increase in the μ_β-value below T_M and T_M decreases with increase in x (figure 2(c)). Thus, the x_c-value of

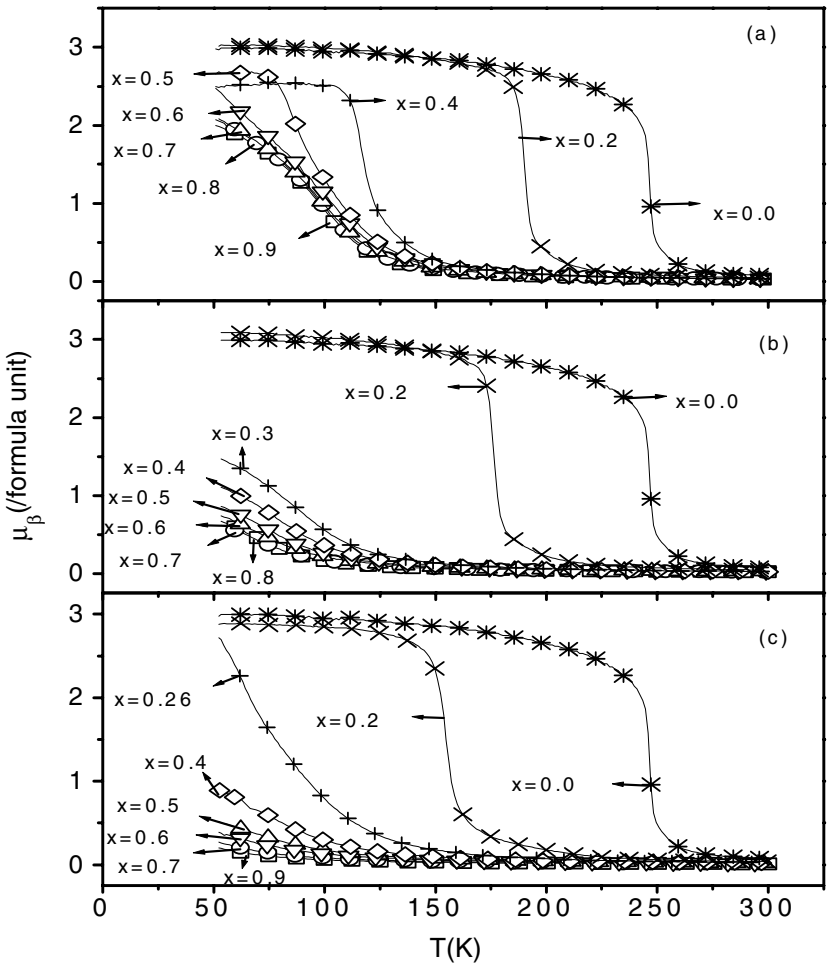

Figure 2. The temperature variation of μ_β in the manganites (a) $(La_{1-x}Nd_x)_{0.7}Ca_{0.3}MnO_3$, (b) $(La_{1-x}Gd_x)_{0.7}Ca_{0.3}MnO_3$ and (c) $(La_{1-x}Y_x)_{0.7}Ca_{0.3}MnO_3$.

$(La_{1-x}Ln_x)_{0.7}Ca_{0.3}MnO_3$ is 0.75, 0.6, 0.3 and 0.2 for Ln = Pr, Nd, Gd and Y respectively, showing a sensitive dependence of x_c on $\langle r_A \rangle$.

The magnetization data for $(La_{1-x}Ln_x)_{0.7}Ca_{0.3}MnO_3$ with Ln = Nd, Gd and Y in the composition range $x \geqslant x_c$ show certain features of significance. Thus, we find that for the compositions close to x_c ($x \sim 0.6$–0.7 when Ln = Nd; $x \sim 0.3$–0.4 in the case of Gd), the low-temperature μ_β-value is significant, reaching values anywhere between 1 and 2.5. It is only when x is very large ($x \gg x_c$) that the μ_β-value decreases to values less than unity. These relatively high values of μ_β, when Ln = Nd and Gd, are probably due to moments of the rare earths. When Ln = Y, the μ_β-values are all low, the highest value of ~ 1 μ_β being observed when $x \sim x_c$ (figure 2(c)). When $x > x_c$, the magnetic moment decreases below 0.5 μ_β. When $x \gg x_c$, the presence of small FM clusters cannot be ruled out, even though the CAF interactions may be dominant. The drastic change in the values of μ_β around x_c in the three series of manganates can be attributed to phase separation due to disorder caused by substitution of the smaller rare-earth cations in place of La. In the Pr system, phase separations

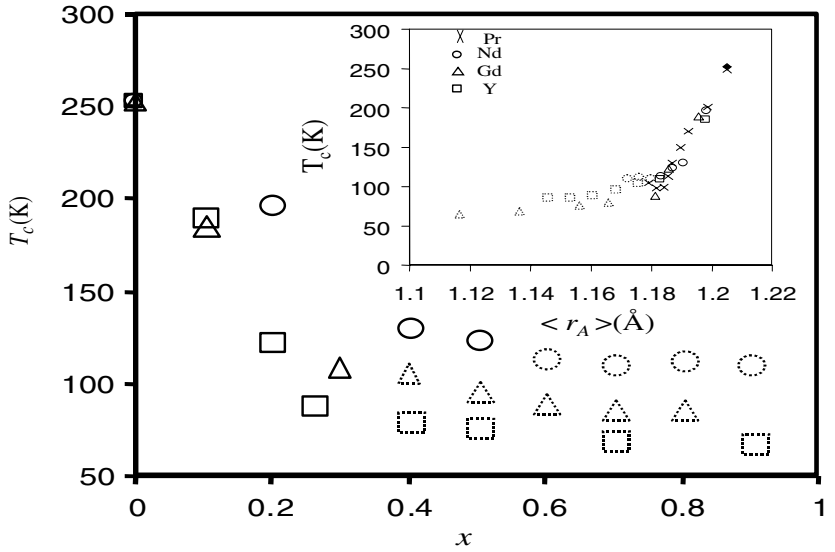

Figure 3. The variation of T_c with x for $(La_{1-x}Ln_x)_{0.7}Ca_{0.3}MnO_3$. Solid symbols represent real T_c and broken symbols represent T_M. The inset shows the variation of T_c with $\langle r_A \rangle$ (Å) for $(La_{1-x}Ln_x)_{0.7}Ca_{0.3}MnO_3$ (the $x = 0$ datum is shown as ♦). $(La_{1-x}Ln_x)_{0.7}Ca_{0.3}MnO_3$ data are taken from [8].

have been reported in the regime of $x \sim x_c$ ($x \sim 0.6$–0.8) [8]. To some extent, the results found here are somewhat comparable to those of de Teresa *et al* [10] who find FMM behaviour at low x and spin-glass behaviour at large x ($\geqslant 0.33$) in $(La_{1-x}Tb_x)_{0.67}Ca_{0.33}MnO_3$.

In figure 3, we have plotted the ferromagnetic T_c of the $(La_{1-x}Ln_x)_{0.7}Ca_{0.3}MnO_3$ composition against x ($x \leqslant x_c$). T_c decreases with increase in x, linearly. In figure 3, we have also plotted the T_M-values of the non-ferromagnetic compositions ($x > x_c$), to show how the T_M-value also decreases with increase in x, albeit with a considerably smaller slope. In the inset of figure 3, we have plotted the values of T_c and T_M against $\langle r_A \rangle$. The T_c-value increases with increase in $\langle r_A \rangle$ for $\langle r_A \rangle \geqslant 1.18$ Å (or $x < x_c$), while T_M increases with $\langle r_A \rangle$ with a smaller slope. The value of $\langle r_A \rangle$ of 1.18 Å marks the critical radius beyond which ferromagnetism manifests itself in $(La_{1-x}Ln_x)_{0.7}Ca_{0.3}MnO_3$. It must be noted that in a variety of manganates of the general composition $Ln_{1-x}A_xMnO_3$, an $\langle r_A \rangle$ of 1.18 Å marks the critical value below which charge ordering becomes robust, rendering it difficult to destroy it by applying magnetic fields or impurity substitutions [11]. An $\langle r_A \rangle$ of 1.18 Å also marks the critical value below which re-entrant FM transitions with $T_c < T_{co}$ are seen [12]. The compositions with $\langle r_A \rangle < 1.18$ Å are AFM insulators. In figure 4, we have plotted μ_β against $\langle r_A \rangle$ for the three series of $(La_{1-x}Ln_x)_{0.7}Ca_{0.3}MnO_3$. The μ_β-values when $\langle r_A \rangle < 1.18$ Å are rather small, well below 3 μ_β, generally less than 1 μ_β. Magnetization in this regime arises from FM interactions in a primarily AFM environment, probably due to the presence of magnetic clusters. Thus, the μ_β-values in the range of 1–2.5 μ_β in figure 4 correspond to the phase separation regime where the values of $\langle r_A \rangle$ are in the 1.18–1.165 Å range. This is consistent with results reported for $(La_{1-x}Pr_x)_{0.7}Ca_{0.3}MnO_3$ system [8]. When $\langle r_A \rangle \leqslant 1.165$ Å, the μ_β-values become considerably smaller, although ferromagnetic interactions due to clusters are likely to be present at low temperatures in this regime as well.

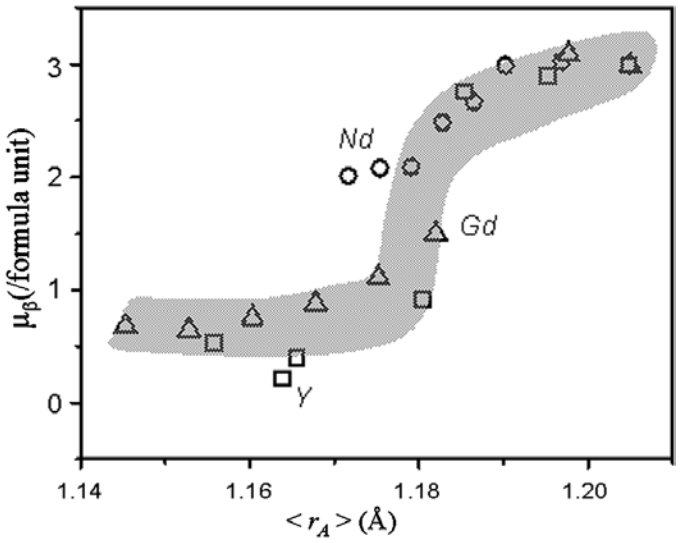

Figure 4. The variation of μ_β with $\langle r_A \rangle$ (Å) in $(La_{1-x}Ln_x)_{0.7}Ca_{0.3}MnO_3$ at 50 K.

The electrical resistivity data for $(La_{1-x}Ln_x)_{0.7}Ca_{0.3}MnO_3$ (Ln = Nd, Gd and Y) reflect the magnetization data, with the $x \leqslant x_c$ compositions showing IM transitions (figure 5). The compositions with $x > x_c$ are insulating and do not exhibit IM transitions. For $x \leqslant x_c$, the value of the resistivity at the IM transition increases with increase in x, and a change in the resistivity of 3–4 orders magnitude is observed at the transition. Thus, the value of resistivity at 20 K for $x \approx x_c$ is considerably higher than that for $La_{0.7}Ca_{0.3}MnO_3$. The temperature of the IM transition, T_{IM}, for $x \leqslant x_c$ compositions decreases linearly with increasing x (figure 6). The T_{IM} versus $\langle r_A \rangle$ plot is linear with a positive slope as expected (see the inset of figure 6). We have not observed any resistivity anomaly at T ($<T_{IM}$) for any of the compositions unlike Uehara *et al* [4] and Deac *et al* [13].

The small but finite magnetic moments and relatively large resistivities at low temperatures found in $(Ln_{1-x}Ln_x)_{0.7}Ca_{0.3}MnO_3$ for Ln = Pr, Nd, Gd and Y around x_c or $\langle r_A^c \rangle$ are a consequence of phase separation. Phase separation also causes thermal hysteresis in the resistivity behaviour around the IM transitions (see the insets in figure 5). The insets in figures 5(a)–(c) show that the resistivity in the warming cycle is lower than that in the cooling cycle up to a certain temperature beyond which the resistivities in the two cycles merge. Upon cooling the sample below the IM transition, the FMM phase grows at the expense of the AFM insulating phase, causing a decrease in the resistivity value. When the same sample is warmed, the insulating phase grows at the expense of the FMM phase, the latter providing the conductive path. The thermal hysteresis in resistivity is therefore due to the percolative conductivity in these manganates, the hysteresis decreasing with increase in $\langle r_A \rangle$ or decrease in x as expected. It must be noted that the compositions with $\langle r_A \rangle > 1.18$ Å which are in a homogeneous FM phase do not show any hysteresis around T_{IM}. Furthermore, the ratio of the peak resistivities in the cooling and heating cycles (ρ_c/ρ_w) is constant for samples with $\langle r_A \rangle > 1.18$ Å in the homogeneous FM regime, but increases significantly with decrease in $\langle r_A \rangle$.

Since phase separation in the $(La_{1-x}Ln_x)_{0.7}Ca_{0.3}MnO_3$ series of manganates is related to size disorder caused by the substitution of small ions in place of La, we have quantitatively examined the effect of size disorder in these manganates, in terms of the size variance of

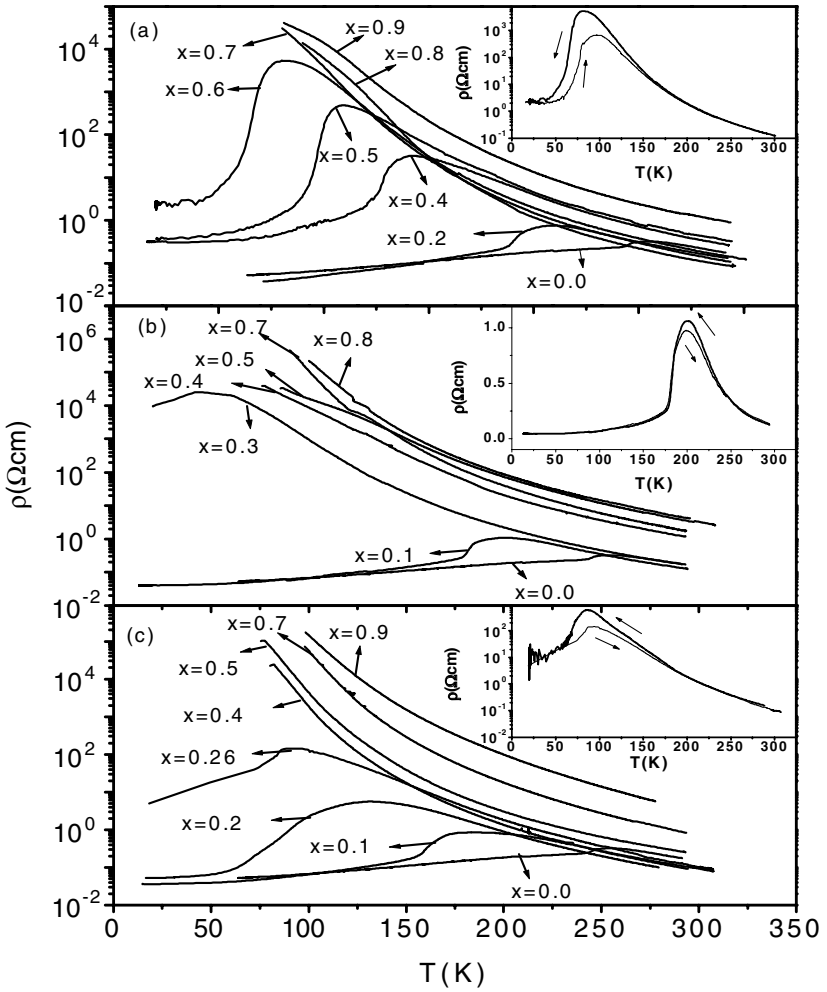

Figure 5. The temperature variation of the resistivity in (a) $(La_{1-x}Nd_x)_{0.7}Ca_{0.3}MnO_3$, (b) $(La_{1-x}Gd_x)_{0.7}Ca_{0.3}MnO_3$ and (c) $(La_{1-x}Y_x)_{0.7}Ca_{0.3}MnO_3$. The curves in the insets show warming cycle data.

the A-site cation radius distribution, σ^2 [14, 15]. For two or more A-site species with fractional occupancies x_i ($\sum x_i = 1$), the variance of the ionic radii r_i about the mean $\langle r_A \rangle$ is given by $\sigma^2 = (\sum x_i r_i^2 - \langle r_A \rangle^2)$. We have examined the electrical and magnetic properties for a series of $(La_{1-x}Ln_x)_{0.7}Ca_{0.3}MnO_3$ with fixed $\langle r_A \rangle$ and variable σ^2. In figure 7, we have shown typical plots of the temperature variation of μ_β for fixed values of $\langle r_A \rangle$ of 1.196 and 1.17 Å. We see a decrease in T_c with increase in σ^2. For $\langle r_A \rangle = 1.17$ Å the material is not ferromagnetic. The μ_β-values as well as T_M show a marked decrease with increase in σ^2. The resistivity decreases with increase in magnetization, and when $\langle r_A \rangle = 1.196$ Å, T_{IM} decreases with increase in σ^2. In figure 8, we have plotted T_c-values of the manganates against σ^2 for compositions with fixed values of $\langle r_A \rangle > 1.18$ Å, along with the T_M-value for fixed values of $\langle r_A \rangle \leqslant 1.18$ Å. Surprisingly, the slopes of the T_c- and T_M-plots are similar ($\sim$9000 K Å^{-2}). The slope of T_c versus σ^2 for $Ln_{0.5-x}La_xCa_{0.5}MnO_3$ compositions, where Ln = Nd and Pr, is reported to be $\sim$15 000 K Å^{-2} [12]. The similarity

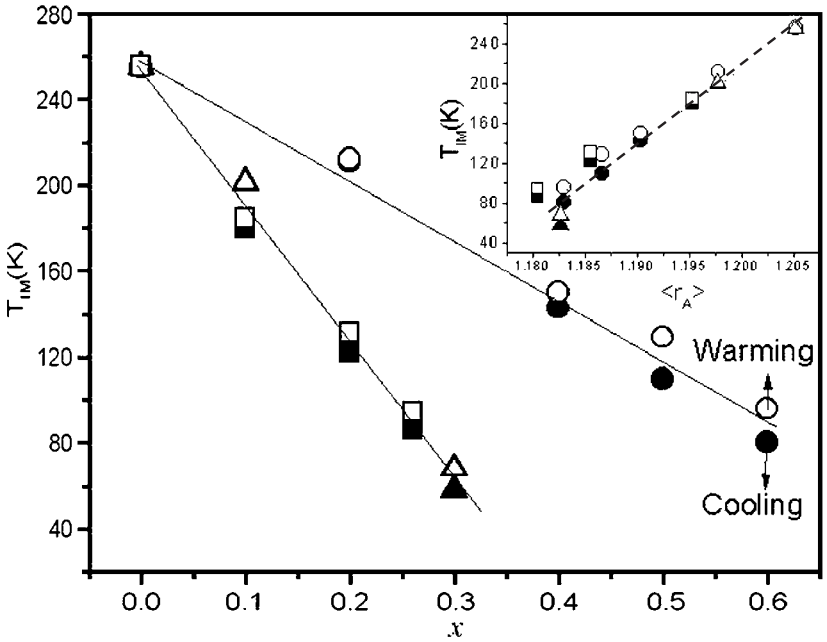

Figure 6. The variation of T_{IM} with x in $(La_{1-x}Ln_x)_{0.7}Ca_{0.3}MnO_3$ for $x \leqslant x_c$. The inset shows the variation of T_{IM} with $\langle r_A \rangle$ (Å) for the same composition range.

in behaviour of these different compositions may be due to presence of ferromagnetic correlations even when $\langle r_A \rangle \leqslant \langle r_A^c \rangle$ or $x > x_c$. By extrapolating the T_c- and T_M-values to $\sigma^2 = 0$, we obtain the intercepts T_c^0 and T_M^0, which represent the transition temperatures in the absence of any size disorder. We have plotted the values of T_c^0 and T_M^0 against $\langle r_A \rangle$ in the inset of figure 8. The values of T_c^0 and T_M^0 increase with increase in $\langle r_A \rangle$ as expected.

As can be seen from figure 5, the resistivities of the $(La_{1-x}Ln_x)_{0.7}Ca_{0.3}MnO_3$ compositions show an a IM transition up to x_c, and these compositions show a significant increase in resistivity with increase in x more prominently than the compositions with $x > x_c$. Electrical conductivity in the $x \approx x_c$ compositions is percolative at low temperatures and, accordingly, we are able to fit the low-temperature data for the compositions with $\langle r_A \rangle > 1.18$ Å to a percolative scaling law, $\log \rho \propto \log |\langle r_A \rangle - \langle r_A^c \rangle|$, as shown in figure 9. The slope of the plot is -2.63, a value close to the experimental and predicted values for percolative systems [3].

We have examined the resistivity data of the insulating compositions with $x > x_c$ in some detail to explore whether they conform to activated hopping defined by $\log \rho \propto 1/T^n$ where $n = 1$, 2 or 4. Here, $n = 1$ corresponds to a simple Arrhenius conductivity. When $n = 2$, the hopping is called nearest-neighbour hopping (NNH). The hopping is controlled by coulombic forces. When $n = 4$, the hopping is termed variable-range hopping (VRH) and the hopping dynamics is controlled by collective excitation of the charge carriers. Figure 10 shows typical fits of the resistivity data for $(La_{1-x}Y_x)_{0.7}Ca_{0.3}MnO_3$ for $x > x_c$. The resistivity data could be fitted to a $T^{-1/2}$-dependence with standard deviations varying from 0.008 to 0.04. The standard deviations for the $T^{-1/4}$-fits were 0.02–0.07. AC conductivity (σ_{AC}) measurements show a frequency dependence of the conductivity, the conductivity increasing with increasing frequency, ω, and decreasing x for a given Ln cation. A fit of σ_{AC} to ω^s gives a value of s in the

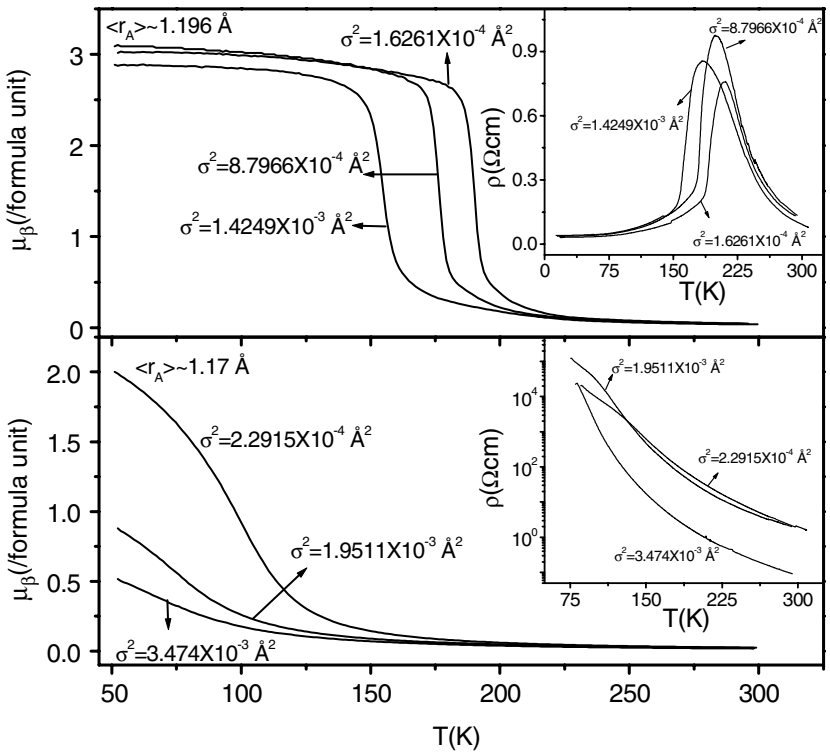

Figure 7. The temperature variation of μ_β in $(La_{1-x}Ln_x)_{0.7}Ca_{0.3}MnO_3$ with (a) $\langle r_A \rangle = 1.196$ Å, (b) $\langle r_A \rangle = 1.17$ Å. The insets show the corresponding variations in resistivities.

range 0.5–0.8, consistent with the VRH mechanism [16]. At high temperatures (>150 K), the conductivity exhibits a frequency independence indicating the dominance of DC conductivity.

In figure 11, we show the temperature response of the real part of the dielectric constant (ε') for $(La_{0.3}Y_{0.7})_{0.7}Ca_{0.3}MnO_3$ at different frequencies. ε' reaches high values at ordinary temperatures but decreases dramatically below ∼120 K. The temperature at which the drop in ε' occurs increases with increasing frequency, exhibiting a relaxor-type behaviour. The dielectric relaxation obtained in the $(La_{1-x}Ln_x)_{0.7}Ca_{0.3}MnO_3$ compositions is similar to that found in copper titanate perovskite dielectrics [17]. The unusually high dielectric constant of $(La_{1-x}Ln_x)_{0.7}Ca_{0.3}MnO_3$ for $x > x_c$ can be understood by assuming the presence of conducting domains surrounded by insulating layers with an activated behaviour of the intra-domain (non-percolative) conductivity. Such a finite conductivity could be one of the reasons for the high dielectric constant beyond 120 K. The dielectric constant at any given frequency decreases with the decrease in conductivity for $x > x_c$ as expected [18]. Similar to the copper titanates, the $(La_{1-x}Ln_x)_{0.7}Ca_{0.3}MnO_3$ ($x > x_c$) compositions exhibit peaks in the dissipation factor which shifts to higher frequencies with increasing temperature. An Arrhenius plot of frequency against temperature gives an activation energy of 68 meV, close to the values for perovskite oxide dielectrics.

4. Conclusions

The present study of the electronic and magnetic properties of three series of rare-earth manganates of the type $(La_{1-x}Ln_x)_{0.7}Ca_{0.3}MnO_3$ where Ln = Nd, Gd and Y, has shown

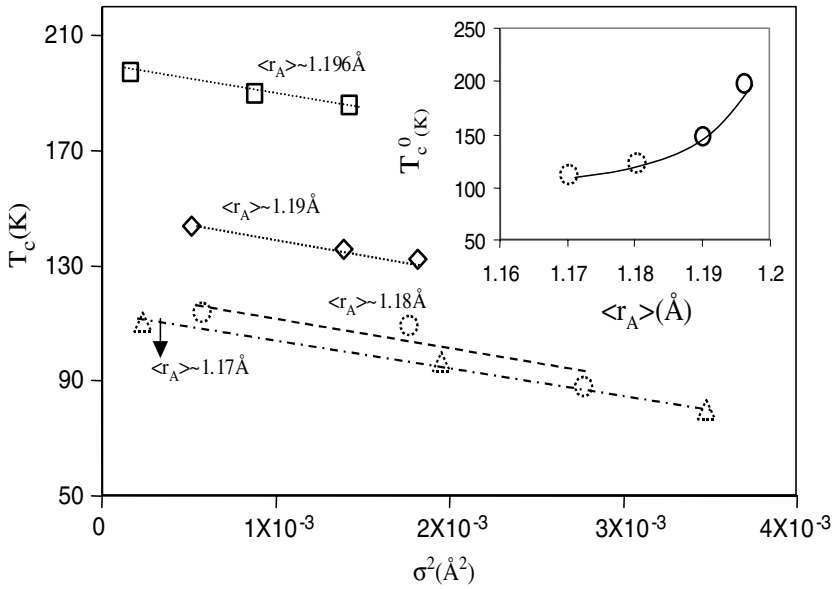

Figure 8. Variations of T_c (solid symbols) and T_M (broken symbols) against σ^2 (Å^2). The inset shows the variation of T_c^0 and T_M^0 against $\langle r_A \rangle$ (Å).

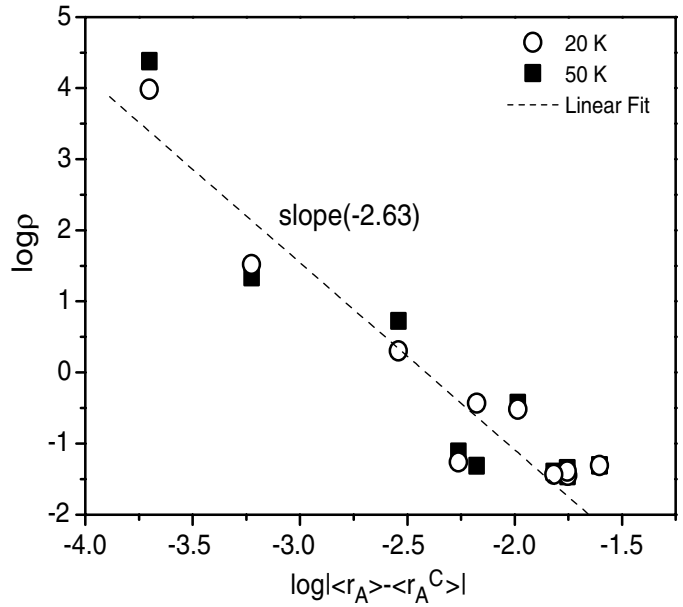

Figure 9. The linear scaling of $\log \rho$ with $\log |\langle r_A \rangle - \langle r_A^c \rangle|$ for $(La_{1-x}Ln_x)_{0.7}Ca_{0.3}MnO_3$ at 20 and 50 K.

that they become ferromagnetic when $x \leqslant x_c$, this change being accompanied by an IM transition. These manganates become AFM insulators when $x > x_c$, but show a small increase in magnetic moment at low temperatures ($T < T_M$). The values of T_c and T_M are both sensitive

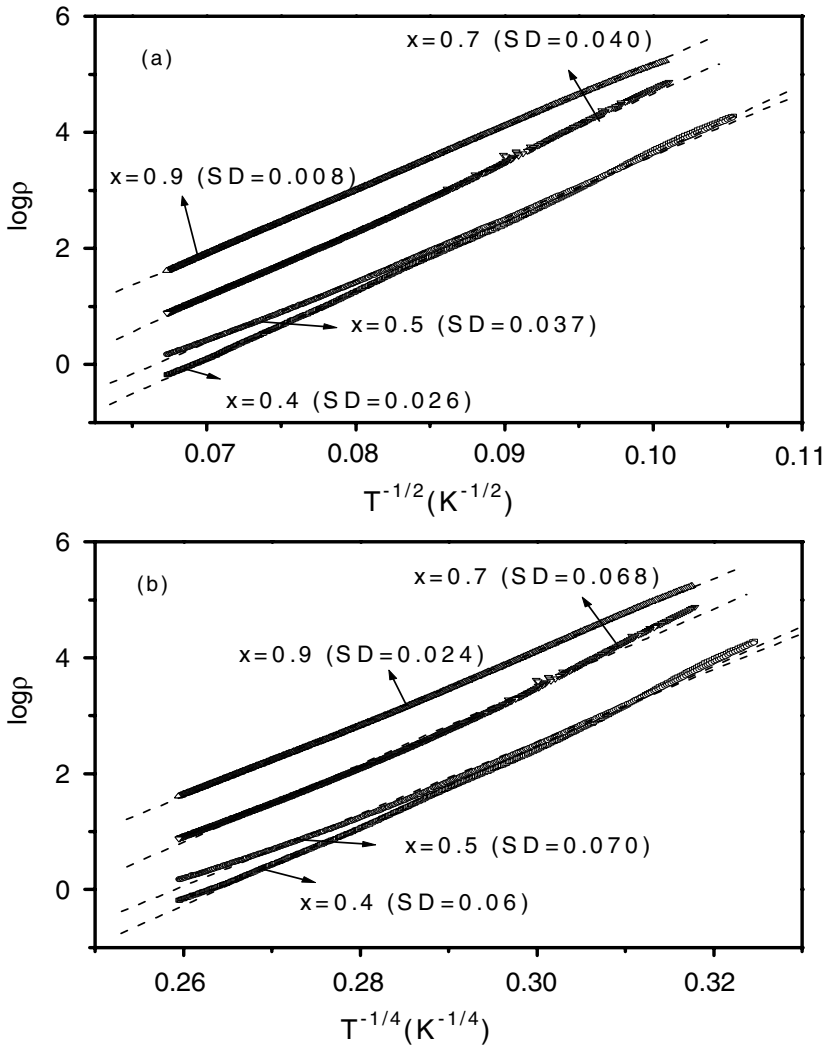

Figure 10. Fits of the resistivity data for $(La_{1-x}Y_x)_{0.7}Ca_{0.3}MnO_3$ for $x > x_c$ to (a) a $T^{-1/2}$-law and (b) a $T^{-1/4}$-law in the 90–220 K range. The open symbols are experimental data points and broken lines represent the corresponding linear fits.

to cation size disorder. The values of x_c are 0.6, 0.3 and 0.2 respectively for Nd, Gd and Y, corresponding to a unique value of the average size of the A-site cation, $\langle r_A \rangle$, of 1.18 Å ($\langle r_A^c \rangle$). It must be recalled that this value of $\langle r_A \rangle$ also marks the critical value below which the ground state is charge ordered. Phase separation is marked around x_c or $\langle r_A^c \rangle$ in all the series of compositions, although ferromagnetic clusters are likely to be present at low temperatures even when $1.0 > x > x_c$. The phase separation in these series of manganates is likely to be triggered by size disorder arising from the substitution of the smaller rare-earth cations in place of La. The results obtained in the present study are consistent with the accepted theoretical models for electronic phase separation in rare-earth manganates and other oxide materials [3, 19, 20].

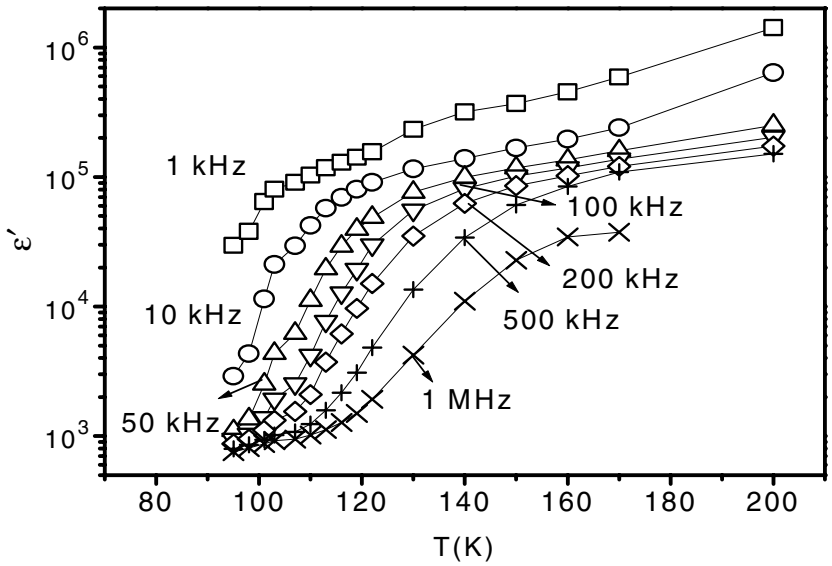

Figure 11. The temperature variation of the real part of the dielectric constant (ε') of $(La_{0.3}Y_{0.7})_{0.7}Ca_{0.3}MnO_3$ at different frequencies.

Acknowledgment

The authors thank BRNS (DAE) for support of this research.

References

[1] Rao C N R and Raveau B (ed) 1998 *Colossal Magnetoresistance, Charge Ordering and Related Properties of Manganese Oxides* (Singapore: World Scientific)
[2] Tokura Y (ed) 1999 *Colossal Magnetoresistance Oxides* (London: Gordon and Breach)
[3] Rao C N R and Vanitha P V 2002 *Curr. Opin. Solid State Mater. Sci.* **6** 97
[4] Uehara M, Mori S, Chen C H and Cheong S-W 1999 *Nature* **399** 560
[5] Babushkina N A, Taldenkov A N, Belova L M, Chistotina E A, Gorbenko O Yu, Kaul A R, Kugel K I and Khomskii D I 2000 *Phys. Rev.* B **62** R6081
[6] Lee H J, Kim K H, Kim M W, Noh T W, Kim B G, Koo T Y, Cheong S-W, Wang Y J and Wei X 2002 *Phys. Rev.* B **65** 115118
[7] Kiryukhin V, Kim B G, Podzorov V, Cheong S-W, Koo T Y, Hill J P, Moon I and Jeong Y H 2000 *Phys. Rev.* B **63** 024420
[8] Balagurov A M, Pomjakushin Y Yu, Sheptyakov D V, Aksenov V L, Fischer P, Keller L, Gorbenko O Yu, Kaul A R and Babushkina N A 2001 *Phys. Rev.* B **64** 024420
[9] Terashita H and Neumeier J J 2001 *Phys. Rev.* B **63** 174436
[10] de Teresa J M, Ibarra M R, García J, Blasco J, Ritter C, Algarabel P A, Marquina C and del Moral A 1996 *Phys. Rev. Lett.* **76** 3392
[11] Rao C N R, Arulraj A, Cheetham A K and Raveau B 2000 *J. Phys.: Condens. Matter* **12** R83
[12] Vanitha P V and Rao C N R 2001 *J. Phys.: Condens. Matter* **13** 11707
[13] Deac I G, Diaz S V, Kim B G, Cheong S-W and Schiffer P 2002 *Phys. Rev.* B **65** 174426
[14] Rodriguez-Martinez L M and Attfield J P 1996 *Phys. Rev.* B **54** R15622
[15] Vanitha P V, Santosh P N, Singh R S, Rao C N R and Attfield J P 1999 *Phys. Rev.* B **59** 13539
[16] Vijaya Sarathy K V, Parashar S, Raju A R and Rao C N R 2002 *Solid State Sci.* **4** 353
[17] Homes C C, Vogt T, Shapiro S M, Wakimoto S and Ramirez A R 2001 *Science* **293** 673
[18] He L, Neaton J B, Cohen M H, Vanderbilt D and Homes C C 2002 *Preprint* cond-mat/0110166
[19] Rao C N R, Vanitha P V and Cheetham A K 2003 *Chem. Eur. J.* **9** 828
[20] Dagotto E, Hotta T and Moreo A 2001 *Phys. Rep.* **344** 1